

---

# A GAME-THEORETIC APPROACH FOR HIGH-RESOLUTION AUTOMOTIVE FMCW RADAR INTERFERENCE AVOIDANCE

---

**Yunian Pan,**  
New York University,  
Brooklyn,  
NY, USA  
yp1170@nyu.edu

**Jun Li**  
NXP Semiconductors,  
San Jose,  
CA, USA  
jun.li\_5@nxp.com

**Lifan Xu**  
The University of Alabama,  
Tuscaloosa,  
AL, USA  
lxu36@crimson.ua.edu

**Shunqiao Sun**  
The University of Alabama,  
Tuscaloosa,  
AL, USA  
shunqiao.sun@ua.edu

**Quanyan Zhu**  
New York University,  
Brooklyn,  
NY, USA  
qz494@nyu.edu

## ABSTRACT

Nonlinear frequency hopping has emerged as a promising approach for mitigating interference and enhancing range resolution in automotive FMCW radar systems. Achieving an optimal balance between high range-resolution and effective interference mitigation remains challenging, especially without centralized frequency scheduling. This paper presents a game-theoretic framework for interference avoidance, in which each radar operates as an independent player, optimizing its performance through decentralized decision-making. We examine two equilibrium concepts—Nash Equilibrium (NE) and Coarse Correlated Equilibrium (CCE)—as strategies for frequency band allocation, with CCE demonstrating particular effectiveness through regret minimization algorithms. We propose two interference avoidance algorithms: Nash Hopping, a model-based approach, and No-Regret Hopping, a model-free adaptive method. Simulation results indicate that both methods effectively reduce interference and enhance the signal-to-interference-plus-noise ratio (SINR). Notably, No-regret Hopping further optimizes frequency spectrum utilization, achieving improved range resolution compared to Nash Hopping.

**Keywords** automotive radar · game theory · frequency hopping · interference mitigation · interference avoidance

## 1 Introduction

High-resolution automotive frequency modulated continuous wave (FMCW) radars have become essential to advanced driver assistance system (ADAS) and autonomous driving (AD) due to their ability to accurately and reliably measure the range, velocity, and angle of targets in all weather conditions [8, 10, 18, 19, 22, 25]. However, the rapid increase in the deployment of automotive radars has led to a growing concern over radar-to-radar interference, where unwanted signals from nearby radars degrade the quality of target detections. To address this, various interference mitigation techniques [6, 9, 11, 12, 20, 21, 23] have been proposed, aimed at enhancing the safety and comfort functions of the automotive radar systems. Depending on the specific automotive radar functions, the necessary improvement in the signal-to-interference-plus-noise ratio (SINR) after interference mitigation varies from a few dB up to infinite. For instance, in radar-based vulnerable road user (VRU) protection applications, any sudden system failure caused by interference is unacceptable, necessitating complete interference avoidance in such critical situations.

Proactive interference mitigation on the transmitter (TX) side [19, 22, 24] is among the most effective techniques for avoiding radar interference. These methods can completely suppress interference by transmitting signals in time slots or subbands where no interference signals are present, thereby ensuring interference-free operation for

safety-critical functions, e.g., adaptive cruise control (ACC), collision mitigation, and VRU protection. For instance, in [17], a technique known as frequency hopping is introduced to mitigate radar interference by rapidly switching the carrier’s starting frequency across a wide range of available subbands. Thus, the likelihood of collisions is reduced. However, the interference problem still prevails as the FMCW radar channel parameters, such as frequency and time offsets, are often randomly assigned without coordination. This lack of structured frequency assignment makes frequency hopping alone insufficient for interference avoidance. Additionally, it limits adaptability in dynamic situations. While improvements can be achieved through techniques like minimum variance beamforming [4], the primary issue stems from improper frequency scheduling. Other proposed solutions involve using communication networks, such as high-bandwidth LTE links, to form radar networks and adopting Medium Access Control (MAC) protocols. These approaches, whether centralized [5] or distributed [3], rely heavily on either a cloud infrastructure or side communication channels, and can be vulnerable to adversarial disruptions.

To develop a more adaptive solution for frequency scheduling, we resort to game theory, modeling radars as players with performance metrics and frequency hopping schemes as their utilities and strategies. In noncooperative game theory, the most common notion is *Nash Equilibrium* (NE) [1], where players have no incentive to deviate from their independent strategies. Another competing notion is *Coarse Correlated Equilibrium* (CCE) [16], which are the “optimal” joint distributions over the players’ hopping strategies, in the sense that the players have no incentive to deviate from the frequency decisions sampled from a CCE.

The concept of NE inherently supports a distributed, incentive-compatible, and stable frequency-hopping solution that may potentially lead to a *system optimum* (SO). However, it presents several limitations in the radar communication scenarios. First, NE is prone to equilibrium selection issues, as players choosing different NE strategies can result in non-equilibrium outcomes; Second, the average radar performance achieved by an NE is not guaranteed to match that of an SO; Third, finding an NE requires either complete knowledge of the environment and other radars—typically inaccessible and computationally intensive (a PPAD-complete problem) [2]—or a learning process with repeated interactions, which does not guarantee convergence. Conversely, convergence to a CCE is more achievable through interactive learning due to the diminishing regrets of individual radars—the analysis of which is well-documented in the literature (e.g., [13, 14]). For this reason, we adopt CCE as the primary solution concept and propose *No-regret Hopping*, an effective distributed frequency scheduling method for avoiding radar interference. Then we compare the *No-regret Hopping* method with a centralized method *Nash Hopping* [15], which targets an NE through model-based learning and also uses the uniformly random strategy as another experimental benchmark. Our simulations indicate that radars with *No-regret Hopping* achieve superior SINR and lower interference rates in interference conditions while improving range resolution by utilizing the available interference-free bandwidth more effectively.

## 2 Problem Formulation

Consider a scenario where a set of FMCW automotive radars, denoted by  $\mathcal{N} := \{1, \dots, N\}$ , experience mutual interference. Each radar transmits linear frequency modulated (LFM) pulses within a total bandwidth  $B$  and starting frequency  $f_c$ . The nonlinear frequency hopping strategy [17] divides the bandwidth  $B$  into  $A$  subbands,  $\mathcal{A} := \{f_1, \dots, f_A\}$ , with each subband defined by a corresponding starting frequency  $f_a = f_c + (a - 1)B_a$  for  $a \in \{1, \dots, A\}$ , and each chirp only sweeps a portion  $B_a$  of the total bandwidth  $B$ .

### 2.1 The Anti-Coordination Game

Consider  $\mathcal{T}$  time frames indexed by  $\tau \in \{1, \dots, \mathcal{T}\}$ , covering a total duration of  $T$ . Each radar  $i \in \mathcal{N}$  transmits  $K^i$  consecutive chirps within each frame. The pulse repetition interval (PRI) is  $T_{\text{PRI}}^i = T/K^i$ , encompassing both active and idle times, where  $(T_{\text{PRI}}^i = T_a^i + T_d^i)$  and  $T_d^i > 0$ . This results in a chirp sweeping slope of  $\alpha^i = B_a/T_a^i$  for radar  $i$ . For simplicity, we assume  $K^i = K$  for all  $i$ . To minimize interference, the radars strategically select channel sequences  $(f_1^i, \dots, f_K^i)$  across the chirps.

Then, the radar-to-radar interference scenario can be modeled as a  $K$ -stage repeated game  $\mathcal{G} = \{\mathcal{N}, \mathcal{A}, \{U_i\}_{i \in \mathcal{N}}\}$ , where the radars, acting as players in  $\mathcal{N}$ , share a common action set  $\mathcal{A}$ . The anti-coordination nature lies in the utility functions  $U_i : \mathcal{A}^N \rightarrow \mathbb{R}$ , where  $f^i, f^{-i} \in \mathcal{A}$  denote the subbands chosen by player  $i \in \mathcal{N}$  and by all other players, respectively. In this paper, the utility function for player  $i$  is defined as:

$$U_i(f^i, f^{-i}) = 10 \log_{10}(\text{SINR}^i(f^i, f^{-i})), \quad (1)$$

where  $\text{SINR}^i(f^i, f^{-i})$  represents the SINR of subband  $[f^i, f^i + B_a]$  at radar  $i$ ’s receiver, based on the selected subband actions  $f^i$  and  $f^{-i}$ . In the absence of interference, the SINR reduces to the signal-to-noise ratio (SNR). If any starting frequency in  $f^{-i}$  matches  $f^i$ , the  $U_i$  decreases, highlighting the anti-coordination objective, as radars aim to avoid overlapping frequencies to maintain higher utility.

## 2.2 Signal Model

Let radar  $i$ 's starting frequency sequence be  $(f_1^i, \dots, f_K^i)$ , and consider  $\mathcal{M} := \{1, \dots, m\}$  targets within its field of view, with range vector  $(r_1^i, \dots, r_m^i)$  and velocity vector  $(v_1^i, \dots, v_m^i)$ . The velocities are negative for approaching targets. The transmitted signal at the  $k$ -th chirp can be expressed as:

$$s^i[t, k] = e^{j2\pi[f_k^i t + \frac{1}{2}\alpha^i t^2]}, \quad 0 \leq t < T_a^i. \quad (2)$$

The received signal reflected from target  $n \in \mathcal{M}$ , after passing through the mixer, can be written as:

$$\begin{aligned} y_n^i[t, k] &= a_n^i s^i[t - \Delta_n^i t_k, k] s^{i*}[t, k] \\ &\approx a_n^i e^{-j2\pi[f_k^i \Delta_n^i t_k + \alpha^i \Delta_n^i t_k t]}, \end{aligned} \quad (3)$$

where  $a_n^i$  is the complex target coefficient.  $\Delta_n^i t_k$  denotes the round trip delay of  $k$ -th chirp reflected from the target and can be approximated by  $\Delta_n^i t_k = \frac{2}{c}(r_n^i + kv_n^i T_{\text{PRI}}^i)$ , where  $c$  is the speed of light.

The true range value can be expressed as

$$r_n^i + kv_n^i T_{\text{PRI}}^i = \bar{r}_n^i + (\epsilon_0 + kv_n^i T_{\text{PRI}}^i), \quad (4)$$

where  $\bar{r}_n^i$  represents the target's coarse range center, with a bin width of  $\frac{c}{2B_a}$ . The fine quantization  $\epsilon_0 \in \left[-\frac{c}{4B_a}, \frac{c}{4B_a}\right]$  has a bin width of  $\frac{c}{2B}$ . Assuming negligible range migration for the coarse range [17], the received target signal in (3) can be rewritten as

$$y_n^i[t, k] = \tilde{a}_n^i e^{-j2\pi f_r t} e^{j2\pi f_d k} e^{-j2\pi\left[\frac{2\bar{r}_n^i}{c} + \frac{2(\epsilon_0 + kv_n^i T_{\text{PRI}}^i)}{c}\right]\Delta b_k^i}, \quad (5)$$

where constant terms are consolidated in the complex target coefficient  $\tilde{a}_n^i$ . Here,  $f_r = \frac{2r_n^i \alpha^i}{c}$  is the coarse range frequency, and  $f_d = -\frac{2v_n^i T_{\text{PRI}}^i f_c}{c}$  is the Doppler frequency. The last term represents the phase compensation across slow time due to frequency hopping, where  $\Delta b_k^i = f_k^i - f_c$  is the known frequency shift at both the transmitter and receiver. Without frequency hopping,  $\Delta b_k^i = 0$ , and a conventional received signal remains; with frequency hopping, the last phase compensation term in (5) allows for higher range resolution. After the received signal is processed through a low-pass filter (LPF) and sampled by an analog-to-digital converter (ADC), the range FFT over index  $t$  extracts the coarse range information. Then, applying a modified Doppler FFT over index  $k$  and nonlinear frequency hopping sequence  $\Delta b_k^i$  enables extraction of both velocity and fine range information [17].

At radar  $i$ 's receiver, assume that the received target signal is mixed with signals directly transmitted by other radars  $\circ \in \mathcal{N}/\{i\}$  with carrier frequencies  $f_k^\circ$ . If  $f_k^\circ = f_k^i$ , the radar-to-radar interference occurs. The demodulated and dechirped interference signal at radar  $i$ 's receiver can be expressed as

$$\begin{aligned} y_n^\circ[t, k] &= a_n^\circ s^\circ[t - \Delta_n^\circ t_k, k] s^{i*}[t, k] \\ &\approx \tilde{a}_n^\circ e^{j\pi(\alpha^i - \alpha^\circ)t^2}, \end{aligned} \quad (6)$$

where  $a_n^\circ$  is the complex interference coefficient and  $\alpha^\circ$  is the chirp slope of radar  $\circ$ . Thus, the dechirped interference signal becomes a new chirp signal with a slope of  $\alpha^i - \alpha^\circ$ . In practice, the start time and frequency of interference depend on factors such as the chirp parameters of both the victim and interfering radars, the position of the interfering radar, and other conditions [9].

By combining the target signal and the interference signal, the received signal at radar  $i$  can be expressed as:

$$\hat{\mathbf{y}}_k^i = \mathbf{y}_k^i + \mathbf{y}_k^\circ + \mathbf{e}_k^i, \quad (7)$$

where  $\mathbf{y}_k^i$  and  $\mathbf{y}_k^\circ$  are the low-pass filtered ADC samples of  $\sum_{n \in \mathcal{M}} y_n^i[t, k]$  and  $\sum_{\circ \in \mathcal{N}/\{i\}, n \in \mathcal{M}} y_n^\circ[t, k]$  within chirp  $k$ , respectively, and  $\mathbf{e}_k^i$  represents the white Gaussian noise.

Let  $P(\cdot)$  denote the average power function of a signal source. The theoretical SINR( $f_k^i, f_k^{-i}$ ) at radar  $i$ 's receiver can be expressed as

$$\text{SINR}(f_k^i, f_k^{-i}) = \frac{P(\mathbf{y}_k^i)}{P(\mathbf{y}_k^\circ) + P(\mathbf{e}_k^i)}. \quad (8)$$

In practice, it requires detection techniques to determine the existence of interference, e.g., the thresholding-based strategy [9], which filters the received signal  $\hat{\mathbf{y}}_k^i$  into an interference component  $\tilde{\mathbf{y}}_k^\circ$  and a clean signal  $\tilde{\mathbf{y}}_k^i$  after interference mitigation. However, due to the stochastic nature of the signals and the lack of visibility into other radars' subband choices, we use a sliding window approach to estimate SNR and SINR periodically for each subband.

The entire hopping process is divided into episodes, with  $\tau := \{k_{\tau-1} + 1, \dots, k_\tau\}$  as the  $\tau^{th}$  episode,  $\tau = 1, \dots, \mathcal{T}$  and  $k_0 = 0$ . For each episode  $\tau$ , we estimate the SINR for each subband  $f$  as:

$$\overline{\text{SINR}}_\tau^i(f) = \frac{1}{\sum_{k \in \tau} \mathbb{1}\{f_k^i = f\}} \sum_{k \in \tau} \frac{\text{P}(\tilde{\mathbf{y}}_k^i) \mathbb{1}\{f_k^i = f\}}{\text{P}(\tilde{\mathbf{y}}_k^i) + \text{P}(\mathbf{e}_k^i)}, \quad (9)$$

whenever interference is detected. When interference-free chirps are present, the SNR can be estimated as:

$$\overline{\text{SNR}}_\tau^i(f) = \frac{1}{\sum_{k \in \tau} \mathbb{1}\{f_k^i = f, \tilde{\mathbf{y}}_k^i = \mathbf{y}_k^i\}} \sum_{k \in \tau} \frac{\text{P}(\mathbf{y}_k^i)}{\text{P}(\mathbf{e}_k^i)} \mathbb{1}\{f_k^i = f, \tilde{\mathbf{y}}_k^i = \mathbf{y}_k^i\}.$$

### 2.3 Frequency Hopping with Mixed Strategy

If each radar occupies a unique subband, no interference occurs across the chirps. However, with multiple subbands available in frequency hopping, only using a single unique subband degrades range resolution, as range resolution is inversely proportional to the total bandwidth utilized. To address this trade-off, we equip each radar  $i$  with an adaptable mixed strategy  $p_\tau^i$  for each episode  $\tau = 1, \dots, \mathcal{T}$ . This strategy is a probability distribution over  $\mathcal{A}$ , i.e.,  $p_\tau^i \in \mathcal{P}(\mathcal{A}) := \{p : \mathcal{A} \rightarrow [0, 1] \mid \sum_{f \in \mathcal{A}} p(f) = 1\}$  for all  $f \in \mathcal{A}$ . Before the start of each chirp  $k \in \tau$ , each radar samples a starting frequency decision, which we will write as  $f_k^i \sim p_\tau^i(\cdot)$  throughout the rest of the paper without explicitly identifying  $\tau$ . In essence, the goal is for radars to employ mixed strategies to generate a sequence of transmitted signals that effectively detect moving targets while balancing the trade-off between range resolution and interference mitigation.

## 3 Solution Concepts and Algorithms

In this section, we present two game-theoretic solution concepts for the anti-coordination game, along with corresponding algorithmic approaches to achieve these solutions during the frequency hopping process.

### 3.1 Nash Equilibrium and Coarse Correlated Equilibrium

Let  $p = (p^i, p^{-i})$  be a mixed strategy profile, it constitutes an NE during every chirp  $k$  if no radar has the incentive to deviate from their own mixed strategy, in the sense of that the expected utility, denoted by  $\bar{U}_i : \mathcal{P}(\mathcal{A}^N) \rightarrow \mathbb{R}$ ,

$$\bar{U}_i(p^i \otimes p^{-i}) := \mathbb{E}_{f^i \sim p^i, f^{-i} \sim p^{-i}} [U_i(f^i, f^{-i})], \quad (10)$$

where  $p^i \otimes p^{-i}$  is the outer product of the players' mixed strategies,  $f$  cannot be improved.

**Definition 1 (Nash Equilibrium (NE))** For the  $K$ -stage repeated game  $\mathcal{G}$ , a mixed strategy profile  $(p^{i,*}, p^{-i,*})$  constitutes a Nash Equilibrium (NE) if for all radars  $i \in \mathcal{N}$ , and all other strategies  $p^i \in \mathcal{P}(\mathcal{A})$ , the following inequalities are satisfied:

$$\bar{U}_i(p^{i,*}, p^{-i,*}) \geq \bar{U}_i(p^i, p^{-i,*}). \quad (11)$$

We denote by  $\mathcal{N}(U)$  the set of NE mixed strategy profiles with  $U$  being the utility functions.

Due to the lack of information about  $U$ , we adopt an *explore-then-commit* type of strategy in Algorithm 1. During Nash Hopping, we partition the chirping horizon  $K$  into an exploration phase  $k = 1, \dots, k_e$ , where the goal is to estimate the channel capacity functions  $U_i$  through uniform mixed strategies; and a commitment phase  $k = k_e + 1, \dots, K$ , where the radars are committed to a mixed strategy Nash equilibrium that maximizes the social welfare.

Nash Hopping requires information exchange even though estimating  $\bar{U}_i$  requires only local interference detection, to compute an NE one needs the utility functions for all radars. This drawback limits its application only to scenarios where information sharing is possible. Besides, achieving an equilibrium state necessitates the coordination of all radars, as the uniqueness of the NE is not guaranteed. Nevertheless, the computational complexity of NE grows exponentially in the number of radars and subbands.

**Definition 2** For the  $K$ -stage repeated game  $\mathcal{G}$ , a joint probability distribution  $\pi \in \mathcal{P}(\mathcal{A}^N)$  is said to be a Coarse Correlated Equilibrium (CCE) if the following equalities are satisfied:

$$\mathbb{E}_{f \sim \pi} [U_i(f^i, f^{-i})] \geq \mathbb{E}_{f \sim \pi} [U_i(f^{i'}, f^{-i})], \quad (12)$$

for all  $f^{i'} \in \mathcal{A}$ . The interpretation is that whenever radar  $i$  deviates from a joint decision  $f$  sampled from a CCE  $\pi$  by choosing some subband  $f^{i'}$ , its expected utility cannot be improved.

---

**Algorithm 1** Nash Hopping
 

---

1: **Input:** Initialize  $p_e^i = \text{unif}(\mathcal{A})$  for all radars  $i \in \mathcal{N}$   
 2: **Output:** Range-Doppler Map of the signals  
 3: **for** exploration chirps  $k = 1 : k_e$  **do**  
 4:     Sample  $f_k^i \sim p_e^i(\cdot)$  for all radars  $i \in \mathcal{N}$   
 5:     **for** each radar  $i$  **do**  
 6:         Send one chirp sweeping subband  $[f_k^i, f_k^i + B_c]$   
 7:         Receive signals and apply thresholding  
 8:         **if** Episode  $\tau$  ends **then**  
 9:             Assign utilities  

$$\tilde{U}_i(f^i, f^{-i}) \leftarrow 10 \log_{10}(\overline{\text{SINR}}_\tau^i(f^i)) \exists j \in \mathcal{N} / \{i\} f^i = f^j$$

$$\tilde{U}_i(f^i, f^{-i}) \leftarrow 10 \log_{10}(\overline{\text{SINR}}_\tau^i(f^i)) \forall j \in \mathcal{N} / \{i\} f^i \neq f^j$$
  
 10:          $(p_e^j, p_e^{-j}) \leftarrow \arg \max_{p \in \mathcal{N}(\tilde{U})} \sum_{i \in \mathcal{N}} \tilde{U}_i$   
 11:         **end if**  
 12:     **end for**  
 13: **end for**  
 14: **for** committing chirps  $k = k_e + 1 : K$  **do**  
 15:     Sample  $f_k^i \sim p_e^i(\cdot)$  for all  $i \in \mathcal{N}$   
 16:     Transmit and receive signals, apply thresholding  
 17: **end for**

---

Compared to NE, Correlated Cooperative Equilibrium (CCE) allows for decentralized solutions. By correlating individual hopping strategies, CCE facilitates coordination, leading to more efficient frequency selection. However, achieving CCE requires a common signaling mechanism, which can be addressed using regret-minimization-based learning.

### 3.2 Regret Minimization and Implicit Regularization

Suppose an interference mitigation scheme generates a sequence  $\{f_k^i, f_k^{-i}\}_{k=1}^K$ . Then, the (external) regret of hopping process for radar  $i$  is, as defined in (13),

$$\mathcal{R}_i = \max_{f^i \in \mathcal{A}} \sum_{k=1}^K [U_i(f^i, f_k^{-i}) - U_i(f_k^i, f_k^{-i})]. \quad (13)$$

This regret notion captures the difference between decisions made and the hindsight optimal. A regret-minimization algorithm allows radars to adapt their frequency hopping strategies over time while minimizing long-term interference.

Algorithm 2 No-Regret Hopping is an epitome of such methods. It ensures that the regret for radar  $i$  remains small, regardless of the decision-making of other radars, and concentrates around its expected value. In the meantime, the exploration parameter  $\gamma_\tau \geq 0$  introduces optimistic biases over the less favored frequency bands, this implicit regularization smooths the distribution  $p_\tau^i$  so that the subbands with lower SINR's will still be chosen, avoiding converging too fast to the pure strategy.

### 3.3 Connection to Coarse Correlated Equilibrium

We hereby discuss the performance guarantee from a theoretical point of view. We start with a well-established result (Lemma 1) from algorithmic game theory [16] to that bridges the regret analysis and the CCE. Let the empirical joint distribution of transmission strategies be

$$\bar{\pi}(f^i, f^{-i}) := \frac{\sum_{k=1}^K \mathbb{1}\{f_k^i = f^i, f_k^{-i} = f^{-i}\}}{K} \quad (16)$$

for all  $(f^i, f^{-i}) \in \mathcal{A}^N$ .

**Lemma 1** *During the hopping process, the empirical joint distribution of frequency hopping strategies  $\bar{\pi}$  within chirp horizon  $K$  is a  $\varepsilon$ -CCE, i.e.,*

$$\mathbb{E}_{f \sim \bar{\pi}} [U_i(f^i, f^{-i})] \geq \mathbb{E}_{f \sim \bar{\pi}} [U_i(f', f^{-i})] - \varepsilon, \quad (17)$$

**Algorithm 2** No-Regret Hopping

- 
- 1: **Input:** For all radars  $i \in \mathcal{N}$ , initialize  $p_1^i = \text{unif}(\mathcal{A})$ , exploration parameter  $\gamma_\tau$ , learning rate  $\eta_\tau$ ,
  - 2: and set loss vector  $\hat{L}_{0,f}^i = 0$  for all  $f \in \mathcal{A}$ ,  $i \in \mathcal{N}$ .
  - 3: **Output:** Range-Doppler Map of the signals
  - 4: **for**  $k = 1 : K$  **do**
  - 5:     **for** all  $i \in \mathcal{N}$  in parallel **do**
  - 6:         Sample subband  $f_k^i \sim p_\tau^i(\cdot)$
  - 7:         Send one chirp sweeping subband  $[f_k^i, f_k^i + B_c]$
  - 8:         Receive signals and apply thresholding
  - 9:         Estimate average  $\overline{\text{SINR}}_\tau^i$
  - 10:     **if** Episode  $\tau$  ends **then**
  - 11:         Update  $\hat{L}_\tau^i$ , for all  $f \in \mathcal{A}$ :

$$\hat{L}_{\tau,f}^i = \hat{L}_{\tau-1,f}^i - \frac{10 \log_{10}(\overline{\text{SINR}}_\tau^i(f))}{p_\tau^i(f)} \quad (14)$$

- 12:     Calculating mixed strategy:

$$\begin{aligned} \tilde{p}_{\tau+1}^i(\cdot) &= \left( \frac{\exp(-\eta_\tau \hat{L}_{\tau,f})}{\sum_{f' \in \mathcal{A}} \exp(-\eta_\tau \hat{L}_{\tau,f'})} \right)_{f \in \mathcal{A}} \\ p_{\tau+1}^i(\cdot) &= (1 - \gamma_\tau) \tilde{p}_\tau^i(\cdot) + \gamma_\tau \text{unif}(\mathcal{A}) \end{aligned} \quad (15)$$

- 13:     **end if**
  - 14:     **end for**
  - 15: **end for**
- 

for all  $f' \in \mathcal{A}$ , if all radars follow the  $\varepsilon$ -no-regret learning dynamics, i.e.,  $\frac{1}{K} \mathcal{R}_i \leq \varepsilon$  for all  $i \in \mathcal{N}$ .

Let  $\mathcal{O}(\cdot)$  be the big-O notation, we present an informal result regarding the performance quantification of Algorithm 2. That is, if each radar  $i$  is following No-regret Hopping, with parameters  $\eta_\tau, \gamma_\tau = \mathcal{O}\left(\sqrt{\frac{\log(A)}{\tau A}}\right)$ , their external regret satisfies  $\mathbb{E}[\frac{1}{T} \mathcal{R}_i] \leq \mathcal{O}\left(\sqrt{\frac{A \log A}{T}}\right)$ . The corollary is that when  $K$  is scaled by  $T$  through a constant, the empirical joint distribution  $\bar{\pi}$  is an  $\mathcal{O}\left(\sqrt{\frac{A \log A}{T}}\right)$ -CCE, which implies the convergence: if we let  $T \rightarrow \infty$ , the empirical distribution gets arbitrarily close to a CCE.

Note that this result is also coupled with a high-probability version, interested readers can refer to online-learning literature such as [7] for formal statements and proofs. In fact, in our specific radar anti-coordination game scenario, the simulations show that in two radar cases, not only the empirical distribution, but the last-iterate joint distribution also converges to the set of CCE.

## 4 Numerical Results

In this section, we examine an interference scenario where two vehicles, each equipped with automotive FMCW radars (Radar 1 and Radar 2), are approaching each other. Both radars employ frequency hopping and apply the proposed game-theoretic frameworks, Nash Hopping and No-Regret Hopping, for sub-band hopping scheduling. The radar parameters are summarized in Table.1.

We consider a challenging interference scenario in which both radars are initially synchronized, with their starting time offsets set to zero. Unlike the theoretical framework, we allow the radars to operate with different PRIs, resulting in a differing number of chirps per frame. However, both radars operate on the same CPI time scale; therefore, Radar 1 updates its mixed strategy every 512 chirps, while Radar 2 does so every 256 chirps. Although this synchronization is enforced for convenience, it is not strictly necessary. As long as the radars gather sufficient information within successive time frames, the strategy update can be unsynchronized.

Table 1: Radar Parameters Configuration

Parameter	Radar 1	Radar 2
subbandwidth (MHz) $B$	150	150
Carrier starting frequency (GHz) $f_c$	77	77
pulse repetition interval ( $\mu s$ ) $T_{PRI}^i$	20	40
Target range ( $m$ ) $r^i$	20	20
Target velocity ( $m/s$ ) $v^i$	-15	15
Number of Chirps per frame $K^i$	512	256
Fast-time sampling per chirp (MHz) $f_s$	450	450
Maximum beat frequency (MHz) $f_b$	22.5	22.5
TX power (dBm)	13	13

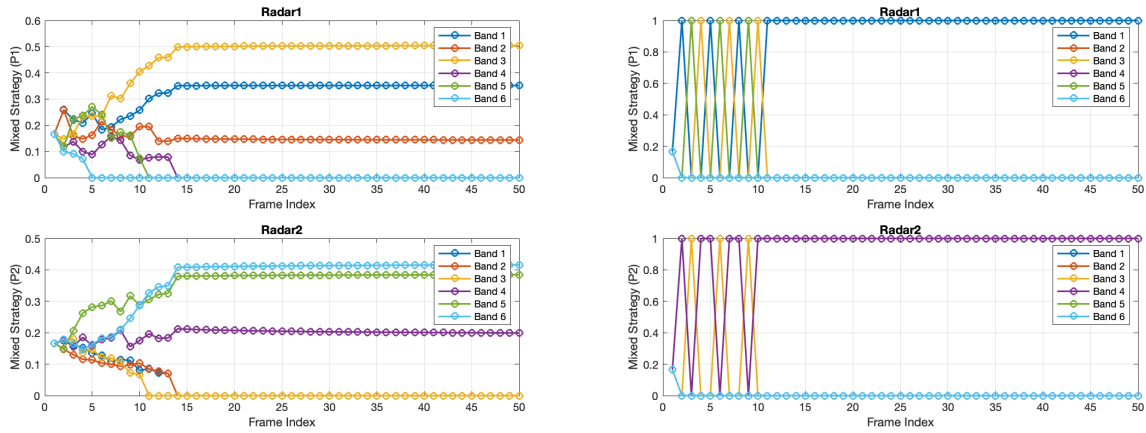


Figure 1: The evolution of mixed strategies for No-Regret Hopping (left), and Nash Hopping (right).

We assume a uniform radar setup, meaning that the algorithms implemented in each radar are identical. Then, we evaluate the two game-theoretic methods, No-Regret Hopping and Nash Hopping, in a scenario with a total bandwidth divided into  $A = 6$  subbands. We plot the evolutions of the mixed strategies  $p_{\tau}^1(\cdot), p_{\tau}^2(\cdot)$  over  $\mathcal{T} = 50$  frames, as well as the frequency-time hopping diagrams for the last frame. In the No-Regret Hopping method, we apply “hard thresholding” to the mixed strategy vectors, setting  $p_{\tau}^i(f) = 0$  for subbands  $f \in \mathcal{A}$  where  $p_{\tau}^i(f) \leq \kappa$ , with  $\kappa$  being a small positive threshold. The probability vector is then renormalized. For Nash Hopping, we consider an exploration phase of 10 time frames, i.e.,  $10 \times K^i$  for radar  $i = 1, 2$ .

As shown in Fig. 1, Nash Hopping effectively eliminates interference after the initial exploration phase. However, due to the presence of multiple pure Nash equilibria, the strategies of the two radars concentrate on two distinct subbands, which evolve randomly within the exploration phase due to the fluctuation of utility estimation. In contrast, No-Regret Hopping produces smoother learning curves, with each radar’s mixed strategy consistently supported by disjoint sets of three subbands. From an interference avoidance perspective, both Nash Hopping and No-Regret Hopping successfully mitigate interference by dynamically scheduling frequency hopping into interference-free subbands. However, Nash Hopping requires inter-radar communication as discussed in Section III, whereas No-Regret Hopping operates independently, without the need for communication between radars.

In Fig. 2, we display the range profiles at the ground truth velocity of  $15m/s$ , using data generated by Nash Hopping and No-Regret Hopping. As a baseline, we include a uniformly random hopping approach, where subbands are randomly sampled with a uniform distribution over all six subbands. Although the uniformly random hopping method achieves the highest range resolution by utilizing all six subbands, it suffers from a high noise floor and low SINR due to accidental interference within each frame. Both Nash Hopping and No-Regret Hopping significantly improve SINR by effectively avoiding interference, as demonstrated in Fig. 1. Moreover, No-Regret Hopping achieves superior range resolution compared to Nash Hopping by utilizing three subbands rather than a single subband, allowing for more efficient use of the available spectrum.

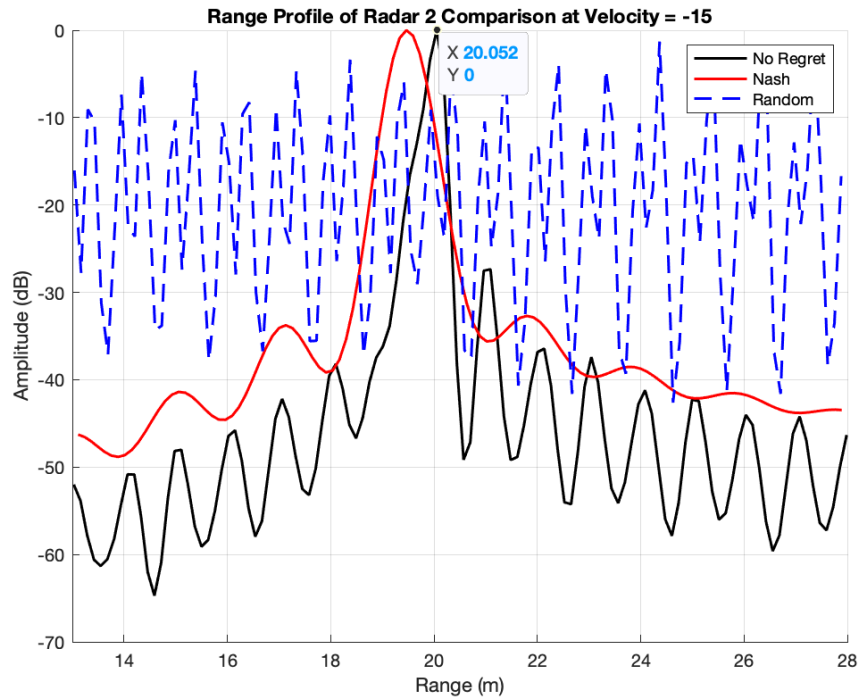


Figure 2: The plots of the range-resolution profile at velocity 15m/s for the three strategies: Nash Hopping, No-Regret Hopping, and uniformly random hopping.

## 5 Conclusion

In this work, we pioneered the application of game-theoretic approaches to mitigate radar-to-radar interference in FMCW automotive radars. By modeling radars as players and leveraging SINR to estimate their utility functions, we propose two frequency hopping strategies: Nash Hopping and No-Regret Hopping. The proposed No-Regret Hopping algorithm, designed to adaptively learn a Coarse Correlated Equilibrium (CCE), demonstrated effective interference avoidance in a decentralized manner, maintaining relatively high range resolution compared to Nash Hopping. Future work will investigate the performance of these algorithms in nonuniform radar setups and enhance their efficiency to meet real-time processing demands.

## References

- [1] T. Başar and G. J. Olsder. *Dynamic Noncooperative Game Theory*. SIAM, 1998.
- [2] C. Daskalakis, P. W. Goldberg, and C. H. Papadimitriou. The complexity of computing a nash equilibrium. *SIAM Journal on Computing*, 39(1):195–259, 2009.
- [3] S. Jin and S. Roy. FMCW radar network: Multiple access and interference mitigation. *IEEE Journal of Selected Topics in Signal Processing*, 15(4):968–979, 2021.
- [4] S. Jin, P. Wang, P. Boufounos, P. V. Orlik, R. Takahashi, and S. Roy. Spatial-domain mutual interference mitigation for MIMO-FMCW automotive radar. *IEEE Transactions on Vehicular Technology*, pages 1–16, 2024.
- [5] J. Khoury, R. Ramanathan, D. McCloskey, R. Smith, and T. Campbell. RadarMAC: Mitigating radar interference in self-driving cars. In *2016 13th Annual IEEE International Conference on Sensing, Communication, and Networking (SECON)*, pages 1–9, 2016.
- [6] F. Laghezza, F. Jansen, and J. Overdevest. Enhanced interference detection method in automotive FMCW radar systems. In *2019 20th International Radar Symposium (IRS)*, pages 1–7, 2019.
- [7] T. Lattimore and C. Szepesvári. *Bandit algorithms*. Cambridge University Press, 2020.



- [8] J. Li, R. Wu, I.-T. Lu, and D. Ren. Bayesian linear regression with cauchy prior and its application in sparse mimo radar. *IEEE Transactions on Aerospace and Electronic Systems*, 59(6):9576–9597, 2023.
- [9] J. Li, J. Youn, R. Wu, J. Overvest, and S. Sun. Performance evaluation and analysis of thresholding-based interference mitigation for automotive radar systems. In *2024 IEEE International Conference on Acoustics, Speech, and Signal Processing Workshops (ICASSPW)*, pages 204–208, 2024.
- [10] M. Markel. *Radar for Fully Autonomous Driving*. Boston, MA: Artech House, 2022.
- [11] J. Mun, S. Ha, and J. Lee. Automotive radar signal interference mitigation using RNN with Self Attention. In *ICASSP 2020 - 2020 IEEE International Conference on Acoustics, Speech and Signal Processing (ICASSP)*, pages 3802–3806, 2020.
- [12] J. Mun, H. Kim, and J. Lee. A deep learning approach for automotive radar interference mitigation. In *2018 IEEE 88th Vehicular Technology Conference (VTC-Fall)*, pages 1–5, 2018.
- [13] Y. Pan, T. Li, and Q. Zhu. On the resilience of traffic networks under non-equilibrium learning. In *2023 American Control Conference (ACC)*, pages 3484–3489. IEEE, 2023.
- [14] Y. Pan, T. Li, and Q. Zhu. On the variational interpretation of mirror play in monotone games. *arXiv preprint arXiv:2403.15636*, 2024.
- [15] Y. Pan and Q. Zhu. Efficient episodic learning of nonstationary and unknown zero-sum games using expert game ensembles. In *2021 60th IEEE Conference on Decision and Control (CDC)*, pages 1669–1676, 2021.
- [16] T. Roughgarden. *Algorithmic Game Theory*, volume 53. ACM New York, NY, USA, 2010.
- [17] Y. Stettiner and N. Arkind. FMCW automotive radar incorporating nonlinear frequency hopping sequence of fractional bandwidth multiband chirps, Mar. 21 2023. US Patent 11,609,303.
- [18] S. Sun, A. P. Petropulu, and H. V. Poor. MIMO radar for advanced driver-assistance systems and autonomous driving: Advantages and challenges. *IEEE Signal Processing Magazine*, 37(4):98–117, 2020.
- [19] S. Sun and Y. D. Zhang. 4D automotive radar sensing for autonomous vehicles: A sparsity-oriented approach. *IEEE Journal of Selected Topics in Signal Processing*, 15(4):879–891, 2021.
- [20] X. Wei, J. Overvest, J. Li, J. Youn, S. Ravindran, and R. J. Van Sloun. Score-based generative modeling for interference mitigation in automotive fmcw radar. In *2024 21st European Radar Conference (EuRAD)*, pages 27–30, 2024.
- [21] R. H. Wu, J. Li, M. Brett, and M. A. Staudenmaier. Radar communication with interference suppression, Nov. 3 2022. US Patent App. 17/245,613.
- [22] L. Xu, S. Sun, K. V. Mishra, and Y. D. Zhang. Automotive FMCW radar with difference co-chirps. *IEEE Transactions on Aerospace and Electronic Systems*, 59(6):8145–8165, 2023.
- [23] J. Youn, J. Li, R. Wu, and J. Overvest. Interference mitigation evaluation methodology for automotive radar. In *2024 21st European Radar Conference (EuRAD)*, pages 115–118, 2024.
- [24] Y. D. Zhang and S. Sun. Identical partitioning of consecutive integer set. In *2024 IEEE 13rd Sensor Array and Multichannel Signal Processing Workshop (SAM)*, pages 1–5, 2024.
- [25] R. Zheng, S. Sun, H. Liu, and T. Wu. Deep-neural-network-enabled vehicle detection using high-resolution automotive radar imaging. *IEEE Transactions on Aerospace and Electronic Systems*, 59(5):4815–4830, 2023.